

Multiscale Modelling of UniMolecular FRET Probes Using Monte Carlo Simulations

Shourjya Sanyal^{1,2}, Donal MacKernan¹, and David F. Coker^{1,3}

¹ CECAM-IRL and School of Physics and Complex Adaptive Systems Laboratory, University College Dublin, Dublin 4, Ireland

² Systems Biology Ireland, University College Dublin, Ireland

³ Department of Chemistry, Boston University, 590 Commonwealth Avenue, Boston, MA 02215, USA

E-mail: shourjya.sanyal@ucdconnect.ie

Abstract. Förster Resonance Energy Transfer (FRET) based biosensors are widely used in experimental biology to understand spatiotemporal dynamics of protein pairs both in-vivo and in-vitro. In our study we have developed an idealised model consisting of two macroparticles, representing proteins attached to fluorescent chromophores, linked with an idealized flexible linker consisting of N point-like beads joined by harmonic springs. Monte Carlo simulations with these models are used to investigate the influence of flexible linkers on unimolecular FRET based bio-sensors. The results provide qualitative insight into the efficacy of designing flexible peptide linkers.

1. Introduction

Genetically encoded FRET bio-sensors are extensively used in molecular biology both in-vivo and in-vitro to observe via optical microscopy, binding between key bio-molecules due to biochemical signals, and thereby deduce, identify and understand biochemical reactions and pathways[1, 2, 3]. Despite the vast variety of forms that such probes take, the basic operating principle is essentially the same. Given a suitable pair of chromophores, when light of an appropriate frequency range is absorbed by the donor, and if the distance r between it and the other chromophore (the acceptor) is sufficiently close (1-10nm)[4], non-radiative energy transfer can take place from the donor to the acceptor[5]. Förster showed that this distance \vec{r} dependent non-radiative energy transfer efficiency E varies as r^{-6} . The corresponding transfer rate is measurable in a variety of ways, including through donor-to-acceptor emission intensity ratios \mathcal{I} , the optical emission intensity of the acceptor, or alteration of donor fluorophore fluorescence lifetime.

The basic structure of the FRET biosensor developed and used in experiment by Komatsu et al[6], that we wish to model, comprises of a ligand domain attached to the donor chromophore, and a sensor domain attached to the acceptor chromophore connected by a flexible linker (see fig. 1.A.). The sensor domain changes its conformation upon perception of a bio-chemical signal. This effectively switches on an attractive interaction between the sensor and ligand domains, increasing the likelihood of their binding and is known as the “ON” state. In absence of the bio-chemical signal there is a lesser likelihood of the two chromophores coming closer and is known as the “OFF” state. FRET based microscopy is feasible provided the FRET sensitised donor-to-acceptor intensity ratio \mathcal{I} in the “ON” state is measurable, and is distinguishably greater



than the “OFF” state basal/background value \mathcal{I}_0 . The performance of a linker is optimized in terms of maximising the signal to noise ratio of those two quantities, defined hereafter as $\Delta\mathcal{I}/\mathcal{I}_0 \equiv \frac{\mathcal{I}-\mathcal{I}_0}{\mathcal{I}_0}$. To increase the measurable \mathcal{I} and \mathcal{I}_0 , the chromophores are joined by suitable peptide linkers of length \mathcal{L} , giving origin to the so called unimolecular FRET bio-sensor systems. Decreasing linker length leads to an increase in both \mathcal{I} and \mathcal{I}_0 , but a decrease in $\Delta\mathcal{I}/\mathcal{I}_0$. The goal of our study is to see if the simplified models can correctly predict values of \mathcal{I} , \mathcal{I}_0 and $\Delta\mathcal{I}/\mathcal{I}_0$.

A great deal of work has succeeded in designing FRET unimolecular probes such as KAR, focused on improving their sensitivity and dynamic range (i.e. $\Delta\mathcal{I}/\mathcal{I}_0$). Allen and Zhang[7, 8], motivated by the desire to track cAMP activity, for example at the plasma membrane, cytoplasm, nucleus, and mitochondria in living cells, systematically optimized probes through circular permutation(cp). Lissandron et al[9] improved cAMP unimolecular probes combining molecular simulation with experiments to optimise linkers through mutation of selective residues, and thereby almost doubled FRET efficiency and substantially improved dynamic range. Pertz et al[10] focusing on the Rho family of GTPases (G proteins) which regulate the actin and adhesion dynamics that control cell migration, developed a fluorescent biosensor to visualize the spatiotemporal dynamics of RhoA activity during cell migration, and subsequently engineered a library of probes[3] by varying several geometrical parameters, such as fluorophore distance (using linkers of different length), dipole orientation (using cp mutants in both the acceptor and donor fluorophores), and sensing module domain topology. This approach accommodated structural constraints imposed by different signaling proteins to produce sensors with increased dynamic range.

The approach of the present paper builds on the probe designs of Komatsu et al[2]. By developing long, flexible linkers ranging from 116 to 244 amino acids in length, they demonstrated that they could optimize the corresponding gain (i.e. the $\Delta\mathcal{I}/\mathcal{I}_0$). Evers et al[11] also investigated similar linker systems made of flexible glycine and serine containing peptide linkers, with enhanced cyan and yellow fluorescent protein terminals (ECFP-linker-EYFP) in which the linker length was systematically varied by incorporating between 1 and 9 GGSGGS repeats. As expected, both steady-state and time-resolved fluorescence measurements showed a decrease in energy transfer with increasing linker length. They also explained how these effects could be quantitatively understood by simple models that describe the flexible linker as a worm-like chain.

The paper is organised as follows. The models, FRET observable and simulation method are detailed in section 2. The simulation results are given in section 3 and compared where appropriate with experimental findings. The conclusions of this work are presented in section 4.

2. Models and Methods

To explore idealized design motifs for chromophore - linker - chromophore systems, we have built simplified models of unimolecular FRET probes, represented by two macroparticles joined by a mechanistic flexible linker (modeling the sort of system investigated by Komatsu et al). One spherical macroparticle represents the donor fluorophore bound to ligand domain, another represents the acceptor fluorophore bound to the signal domain. We use the Monte Carlo simulation approach introduced by Metropolis et al[12, 13] to explore the statistical properties of each model.

The spherical macromolecules interact through a pair potential of the form $V(\vec{r}_1, \vec{r}_2) = V_s(\vec{r}_1, \vec{r}_2) + V_\ell(\vec{r}_1, \vec{r}_2)$, where the first term denotes binding between the macroparticles due to a biochemical signal, and the second term an interaction specific to each linker type. When the signal domain is in “ON” state, V_s is represented by an attractive square well interaction of depth ϵ for $\sigma < r < \sigma + \Delta$, where $r = |\vec{r}_2 - \vec{r}_1|$. When the signal domain is in the “OFF” or basal state V_s is set uniformly to zero.

The protein diameter defined as σ will hereafter be used as a measure of length and the

equivalent of $\sim 24\text{\AA}$ representing the diameter of the Fluorescent Proteins. The Föster Radius R_0 is assumed to be 2.5 times larger than σ [14], and the macroparticles in the “ON” state interact within a narrow attractive well Δ of width 0.5σ . In our models the distance dependence of the FRET efficiency is approximated by the expression $E(r) = \frac{1}{1+(r/R_0)^6}$ [5]. The binding in the “ON” state is measured in terms of ϵ . Energy is measured in terms of $k_B T$ and in this units $\epsilon\sigma^2/k_B T = 1$ can be equivalently written as $\epsilon = 1k_B T$.

2.1. Bead and Spring linker

In the case of the bead and spring linker model the macroparticles are joined by a discrete chain made of N point-like beads at position $r_i, i = 1, \dots, N$. These point particles are connected to the macroparticles and among themselves by harmonic springs, and interact with a simple isotropic pair potential [15].

$$V_\ell = V_{chain} = \frac{1}{2}k_s[|r_1 - R_1| - d_1]^2 + \sum_{i=1}^{N-1} \frac{1}{2}k_s[|r_{i+1} - r_i| - d_0]^2 + \frac{1}{2}k_s[|R_2 - r_n| - d_1]^2 \quad (1)$$

The equilibrium distance d_0 between successive beads along the chain is assumed to be 3.8\AA corresponding to the distance between two C_α atoms in a peptide. The equilibrium distance d_1 between the macroparticle and the bead is defined as sum of radius of the macroparticle and the bead i.e. 13.9\AA . We set the spring constant $k_s = 80$ in the units of $k_B T$. This value of k_s was chosen to reproduce experimentally observed values of FRET intensity as a function of number of residues.

2.2. Bead and Spring linker with Bending Forces

These models consider an additional bending contribution attributed to triplets of consecutive beads in a chain, $V_\ell = V_{chain} + V_{bend}$ where the reference bend angle $\phi_0 = 116^\circ$ often used to model angular bonds between two C_α atoms in a peptide [16].

$$V_{bend} = \frac{1}{2}k_{bend} \sum_{i=2}^{N-1} [\cos\phi - \cos\phi_0]^2 \quad (2)$$

where

$$\cos\phi = \frac{(r_{i+1} + r_i) \cdot (r_{i-1} + r_i)}{|r_{i+1} + r_i||r_{i-1} + r_i|} \quad (3)$$

2.3. Effective potential linker

These macroparticles interact with a simple isotropic pair potential,

$$V_\ell(|\vec{r}_2 - \vec{r}_1|) = \begin{cases} 0 & \text{if } r > \sigma \text{ or } r < L \\ \infty & \text{otherwise} \end{cases} \quad (4)$$

Geometrically this can be visualized as two non-overlapping particles free to move inside a sphere of diameter L .

3. Results

3.1. Flexible Linker systems

Simulations have been carried out for systems of two macroparticles linked by a harmonic chain of $10 \leq N \leq 250$ discrete beads, each of them qualitatively representing an amino acid unit in the linker peptide [17]. All systems have been equilibrated for 10^7 Monte Carlo moves, and

statistics have been collected over an equal number of steps. The binding energy ϵ representing attractive potential between the macroparticle has been varied over the range $0 \leq \epsilon/k_B T \leq 6$. A remarkable correspondence between the experimentally observed behavior and the bead and spring linker is presented in the Fig.1.B. Where the 0ϵ represents the “OFF” or basal state, and the binding energy in the case of “ON” state is predicted to be 2.5ϵ . This illustrates the possibility to predict the complex protein - linker - protein system using such simple models.

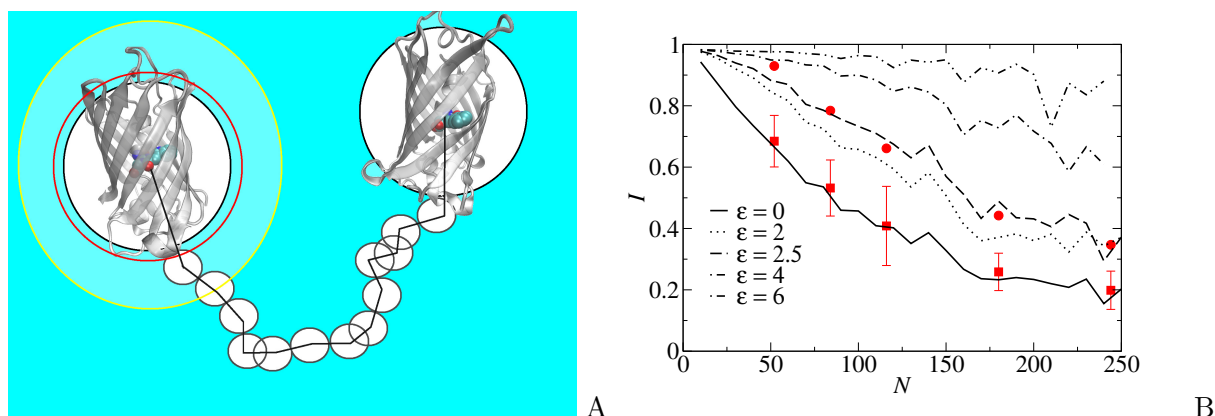


Figure 1. (A) Schematic representation of the unimolecular FRET probe with flexible linker used in experiment reported by Komatsu et al. (B) FRET sensitised donor-to-acceptor intensity ratio of the flexible linker model as a function of number of linker residues. Results presented are for the model “OFF” state I_0 (full line, black), and in the “ON” state I for four different values of the macroparticle interaction strength ϵ . Experimental data from Komatsu et al[6], in the “OFF” or basal state (filled red squares) and in the “ON” state (filled red circles) are superimposed on the theoretical predictions.

In order to compare the bead and spring linker with the effective potential linker, similarities in configuration space is illustrated by plotting the end to end distribution of the macroparticles in the basal or “OFF state for the four linker lengths as shown in Fig.2.A. Our simulation shows that the linker length N in the case of the bead and spring linker, can be mapped to the sphere diameter L (in the case of effective linker potential) using a simple relation $N \sim 40L - 70$

3.2. Effects of Binding Energy ϵ

The thermodynamics state of the system is characterised primarily by the mean square distance between the macroparticles, and by the equilibrium fluctuation of this same quantity. The major feature revealed by this figure is the transition from a Gaussian chain at low ϵ , to a closed ring at high value of ϵ as shown in Fig.2.B. In the former case, the average separation scales like $N^{\frac{1}{2}}$, in agreement with well-known universal properties of Gaussian chains, in the second case the average distance is independent of N . As shown in Fig.1.B. the FRET sensitised donor-to-acceptor intensity is low in the open chain regime, and high when the system is in the ring configuration. As a result, the intensity monotonically increases with increasing ϵ , and decreases with increasing N , at a rate that increases with decreasing ϵ .

3.3. Effects of Bending and Torsion Forces on Chain Dynamics

The addition of a weak bending term k_{bend} does not change significantly the end-to-end distribution and thus the FRET results, as shown in Fig.3.A. Simulations have been carried

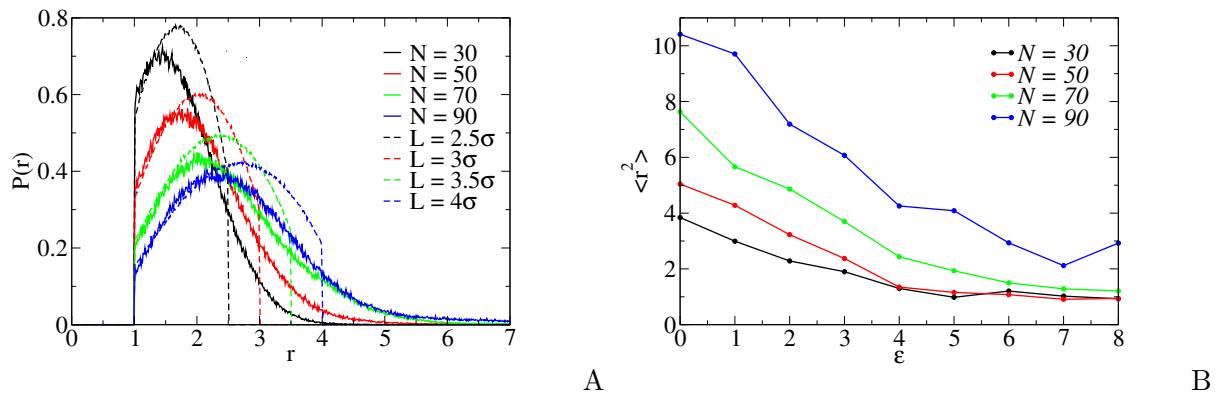


Figure 2. (A) Distribution of end-to-end distances in the “OFF” case for the bead and spring (full line) and the effective potential linker (dashed line). (B) Mean square displacement as a function of binding energy ϵ for the bead and spring linker.

out with $k_{bend}/k_B T = 40$, corresponding to a relatively weak perturbation of the harmonic chain. A few simulations with higher k_{bend} values have confirmed the insensitivity of the results on the choice of k_{bend} . The insensitivity of the end-point distribution to bending is consistent with general results on the structural and thermodynamic properties of Gaussian chains [18].

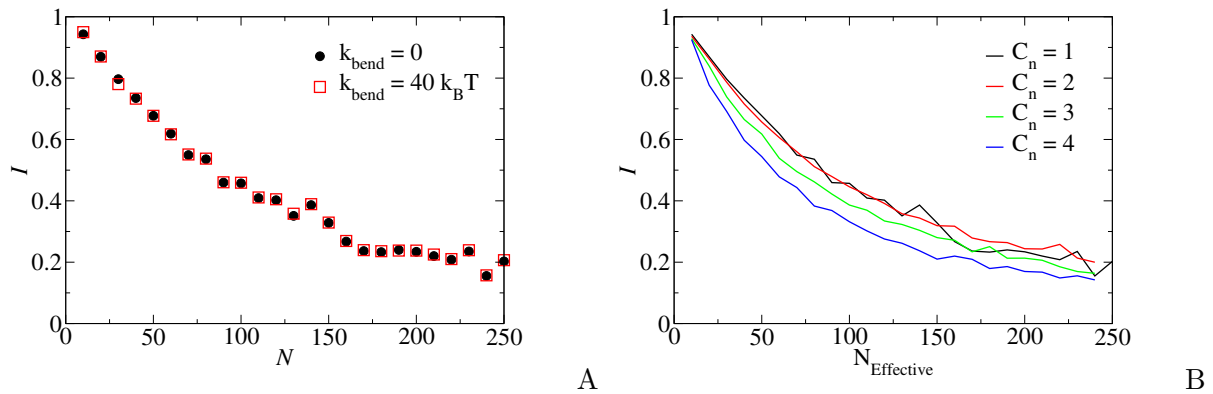


Figure 3. (A) FRET sensitised donor-to-acceptor intensity ratio in the “OFF” case as a function of linker length for a bead and spring linker with bending energy term ($k_{bend}/k_B T = 0$, filled black dots) and ($k_{bend}/k_B T = 40$, empty red squares). (B) FRET sensitised donor-to-acceptor intensity ratio in the “OFF” case as a function of effective linker length for a for a bead and spring linker with varying C_n from 1 to 4.

3.4. Relation between the Characteristic Ratio C_n and Spring Constant k_s

Two different approaches are widely used to model flexible polymer systems. On one hand there is the worm like harmonic chain with uniform flexibility determined by a spring constant k_s , and the segmentally flexible chain [19, 20] where the segment size is determined by the characteristic

ratio C_n . In Fig.3.B. we have used the same effective linker length $N_{Effective}$ of 240 residues but varied the segment size from $C_n = 1$ at $N = 240$ to $C_n = 4$ at $N = 60$. As increasing the value of spring constant k_s gives higher FRET sensitised donor-to-acceptor intensity, the results show that by increasing the characteristic ratio C_n one can increase the effective spring constant k_s .

4. Conclusions

The idealised nature of the models used in this study implies that our observations and conclusions might have fairly general validity. The simulation results show that the bead and spring model linkers are able to reproduce the experimental properties of unimolecular FRET probes. The agreement between experiment and simulation suggests that this approach could be used to predict experimental values of binding energy between the ligand and signal domain. Since these effects are due to configuration phase properties, the results of the bead and spring model can be reproduced by the simple effective potential linker model.

Acknowledgments

Acknowledgments Support from SimSci (Funded under the programme for Research in Third-level Institutions and co-funded Under the European Regional Development Fund) (S.S), Systems Biology Ireland, Dublin (S.S), and SFI Grant No.08-IN.1-I1869 (D.M.K) is acknowledged. The authors thank Pietro Ballone for his insightful contributions to this work .

References

- [1] Miyawaki A 2003 *Dev. Cell.* **4** 295-305
- [2] Miyawaki A 2011 *Annu. Rev. Biochem.* **80** 357-73
- [3] Fritz RD, Letzelter M, Reimann A, Martin K, Fusco L, Ritsma L, Ponsioen B, Fluri E, Schulte-Merker S, van Rhee J and Pertz O 2013 *Sci. Signal.* **6** rs12
- [4] Berney C and Danuser G 2003 *Biophys. J.* **84** 3992-4010
- [5] Lakowicz J R 2010 *Principles of Fluorescence Spectroscopy* vol 3 (New York : Springer) pp 443-72
- [6] Komatsu N, Aoki K, Yamada M, Yukinaga H, Fujita Y, Kamioka Y and Matsuda M 2011 *Mol. Biol. Cell.* **22** 4647-56
- [7] Allen MD and Zhang J 2006 *Biochem. Biophys. Res. Commun.* **348** 716-21
- [8] Zhang J and Allen MD 2007 *Mol. Biosyst.* **3** 759-65
- [9] Lissandron V, Terrin A, Collini M, D'alfonso L, Chirico G, Pantano S and Zaccolo M 2005 *J. Mol. Biol.* **354** 546-55
- [10] Pertz O, Hodgson L, Klemke RL and Hahn KM 2006 *Nature* **440** 1069-72
- [11] Evers TH, van Dongen EM, Faesen AC, Meijer EW and Merckx M 2006 *Biochemistry* **45** 13183-92
- [12] Metropolis N, Rosenbluth A W, Rosenbluth M N, Teller A H and Teller E 1953 *J. Chem. Phys.* **21** 1087-92
- [13] Frenkel D and Smit B 1996 *Understanding Molecular Simulation: From Algorithms to Applications* vol 1 (Orlando, USA: Academic Press) chapter 2 pp 23-58
- [14] Hink M A, Visser N V, Borst J W, van Hoek A and Visser A J W G 2003 *J. Fluoresc.* **13** 185-187
- [15] Strobl G 2007 *The Physics of Polymers* (Berlin Heidelberg : Springer-Verlag)
- [16] Bereau T and Deserno M 2009 *J. Chem. Phys.* **130**
- [17] Caracciolo S, Parisi G and Pelissetto A 1994 *J. Statist. Phys.* **77** 519-543
- [18] de Gennes P G 2007 *Journal of Polymer Science: Polymer Symposia* **61** 313-15
- [19] Yguerabide J, Epstein H F and Stryer L 1970 *J. Mol. Biol.* **51** 57388
- [20] Garca de la Torre J, Pérez Sánchez HE, Ortega A, Hernández JG, Fernandes MX, Díaz FG and López Martínez MC 2003 *Eur. Biophys. J.* **32** 477-86